# 22.315 - Homework 2

**Name:** Lorenzo Mazzocco **Due Date:** March 9 2023
**Code:** StarCCM+

## Contents

# 1. INTRODUCTION

This homework is based on the study of a particular flow field: the Taylor-Green Vortices (TGV). This flow was introduced by G.I. Taylor and A.E. Green in their 1937 paper "*Mechanism of the Production of Small Eddies from Large Ones*" as a mathematical tool to study how large eddy structures decay into progressively smaller structures due to the viscosity of the fluid. Solving the Navier Stokes equations for TGV initial conditions gave them insights on the validity of (semi)empirical correlations derived in wind tunnel experiments.

The goal of this homework is to study the evolution of the same large eddy structures but in a completely different setting: an inviscid flow. In theory with zero viscosity the flow field should be conserved in time but numerical methods can, and most often do, introduce fictitious diffusion or overshooting while interpolating between mesh cells in space and also in time.

We construct an experiment matrix to get insight on how different spatial interpolation methods and different meshes introduce numerical errors in the time evolution of the field. We monitor the conservation of the total kinetic energy of the flow domain as our main indicator of flow conservation.

# 2. GEOMETRY AND BOUNDARY CONDITIONS

The domain is a simple 2D square defined by $x \in [-\pi, \pi]$ and $y \in [-\pi, \pi]$.

Insight about the boundary conditions are given by the second paper provided for this homework (M. Brachet et al, "*Small-scale structure of the Taylor-Green vortex*"). In §2 they describe the characteristics of the initial velocity field, which shows periodicity in boxes of side-lenght of $2\pi$ with 4 mirrored vortices of side-length $\pi$ which do not exchange mass between each other. Because of this the authors would call our entire domain *periodicity box* and the 4 quarter geometries *impermeable boxes*.
Coherently with the characteristics of the flow field the boundary conditions for all 4 of the domain sides are selected to be **symmetry boundary conditions**.

# 3. FLOW INITIALIZATION

## 3.1. Velocity and Pressure Initialization

Initial conditions are given in both papers for the TGV velocity field. The most general form for 3D incompressible flow is characterized by a single mode:

$$v_x(r, t=0) = \frac{2}{\sqrt{3}} sin\left(\theta + \frac{2\pi}{3}\right) sin(x)cos(y)cos(z) \tag{3.1}$$

$$v_y(r, t=0) = \frac{2}{\sqrt{3}} sin\left(\theta - \frac{2\pi}{3}\right) sin(y)cos(x)cos(z) \tag{3.2}$$

$$v_z(r, t=0) = \frac{2}{\sqrt{3}} sin(\theta)cos(x)cos(y)sin(z) \tag{3.3}$$

The flow was selected for $z = 0$ and $\theta = 0$, yielding a simple field:

$$v_x(r, t = 0) = sin(x)cos(y) \tag{3.4}$$

$$v_y(r, t = 0) = -cos(x)sin(y) \tag{3.5}$$

The field is visualized in figure 3.1:

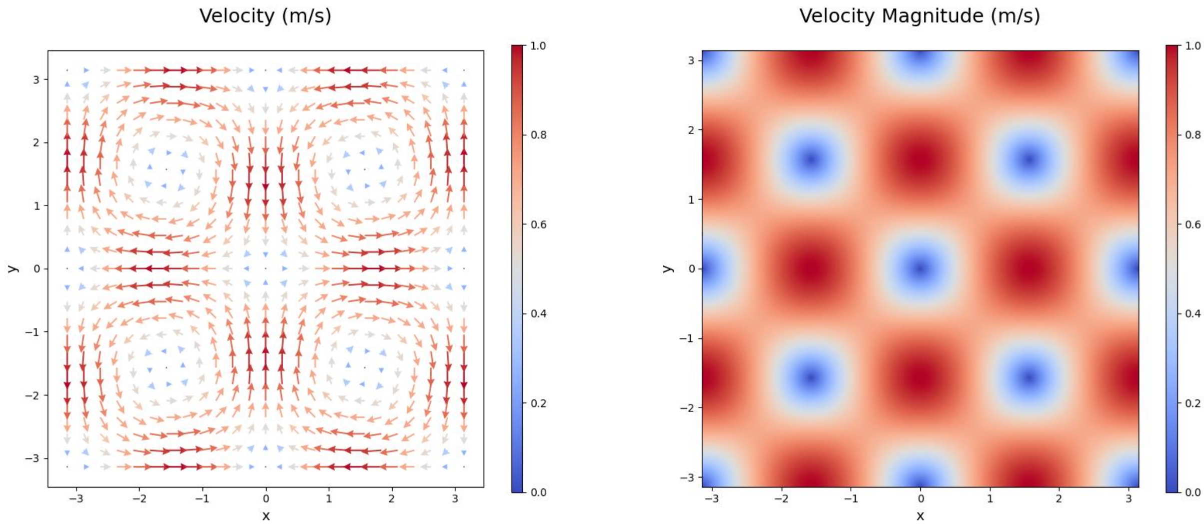

Figure 3.1: Velocity field initialization

Once the velocity field is set one can compute the associated pressure field solving the 2D equations of momentum conservation for inviscid flow (a full derivation can be found in Appendix A). The resulting pressure function is:

$$P(x, y) = \frac{\rho}{2}\left[cos^2(x) + cos^2(y)\right] \tag{3.6}$$

The pressure field can be visualized in figure 3.2:

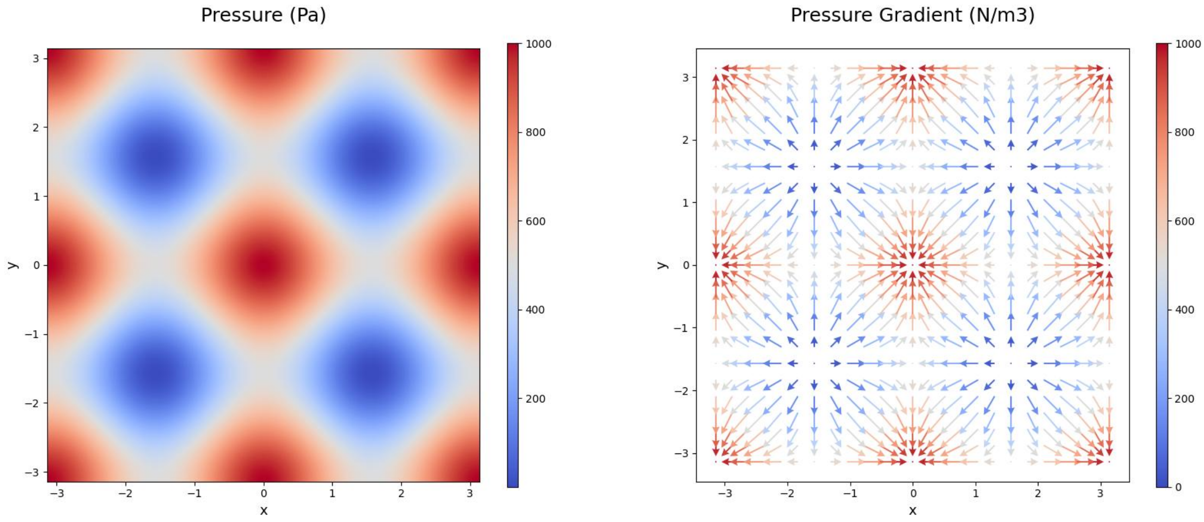

Figure 3.2: Pressure field initialization

## 3.2. On the Importance of Correct Pressure Initialization

How important is it to initialize the pressure field correctly? In theory when we use a segregated solver the pressure initialization shouldn't matter at all because when computing the first timestep the solver will perform enough iterations to converget to the right pressure distribution anyway. Nevertheless it is important to verify this convergence before-hand if one does not initialize the pressure field correctly.

For example when using a precise convective interpolator (like MUSCL) the numerical diffusion is small and the relative effect of a bias caused by wrong pressure initialization can become noticeable. I tested how big of an error we introduce when initializing the pressure field to be constant (0 Pa) vs the correct pressure function for different time advancement schemes. We simulated up to 0.4s using a MUSCL convective interpolator. The results are found in 3.3:

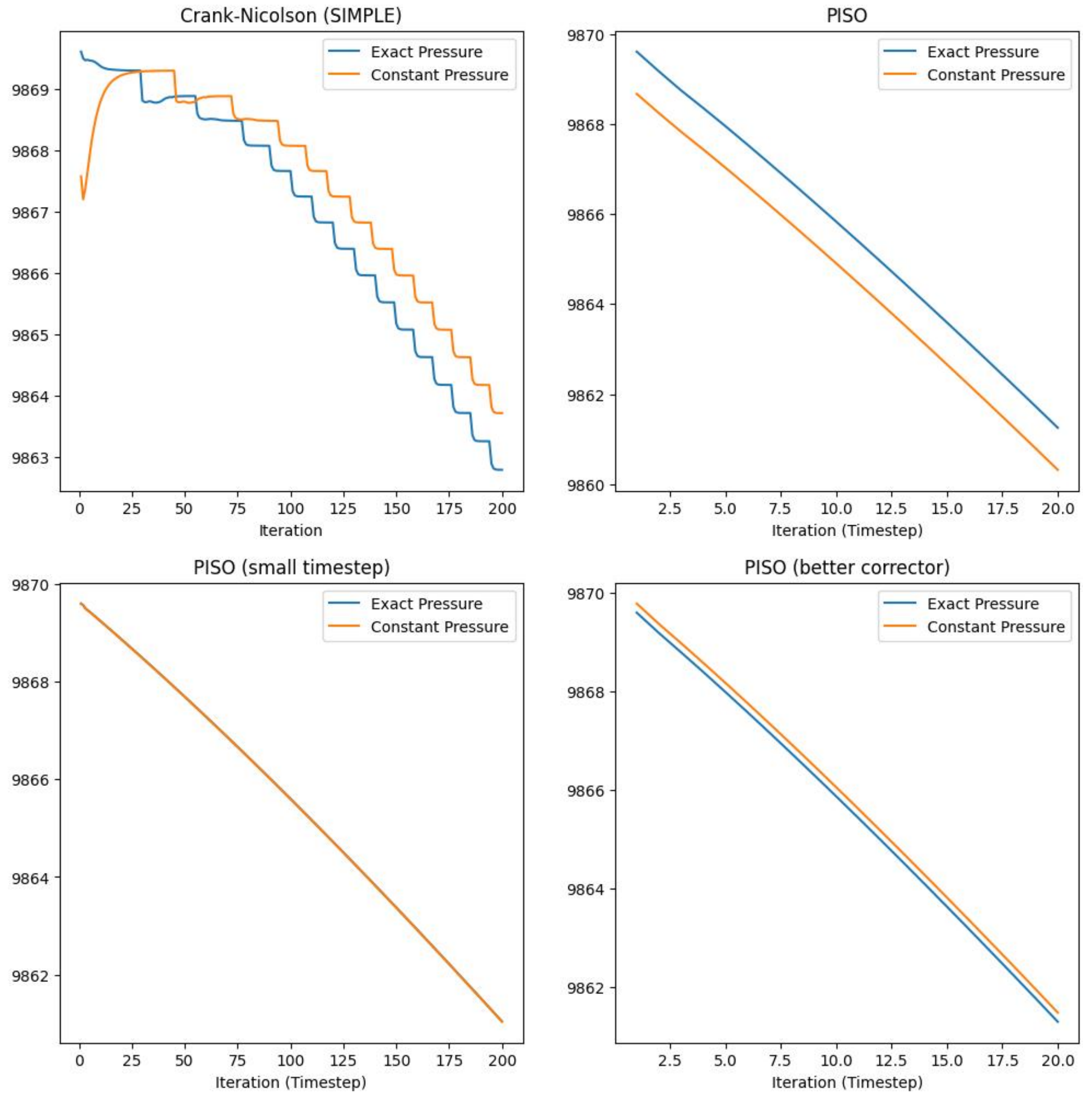

Figure 3.3: Pressure initialization bias. The figure shows the evolution of total domain kinetic energy (J) as a function of iteration. Top-left is a 2nd order implicit scheme (0.02s timestep). Top-right is PISO (0.02s timestep, 0.25 residual reduction). Bottom-left is PISO (0.002s timestep, 0.25 residual reduction). Bottom-right is PISO (0.02s timestep, 0.001 residual reduction)

We notice that the implicit method (Crank Nicolson with inner SIMPLE iterations) is slower to converge but it does not introduce an error (both initializations converge to the same value for each timestep). On the other hand the PISO scheme introduces a significant bias which can be reduced lowering the timestep or requiring more stringent convergence criteria on the inner iterations of the scheme.

# 4. TIME ADVANCEMENT SCHEME AND CONVERGENCE CRITERIA

The only time advancement scheme used in this homework is the **2nd order implicit scheme**. This solver is a Crank-Nicolson scheme with inner iterations of the SIMPLE segregated solver to solve implicit Navier Stokes equations at every timestep. The step advancement follows:

$$\frac{u_i^{(n+1)} - u_i^{(n)}}{\Delta t} = \frac{1}{2}\left[F_i^{(n+1)} + F_i^{(n)}\right]$$

As the name suggests the Crank-Nicolson time-advancement scheme guarantees both stability (implicit) and 2nd order accuracy.

Given that the goal of this homework is to compare meshes and interpolation schemes and not time-advancement schemes, rigorous convergence criteria were imposed on the solver to avoid introducing any numerical error through bad solver iterations. I used two criteria to verify the convergence of the total KE in the domain at every time-step:

1. **Asymptotic Limit**: $|$Max - Min$|$ $<$ 1E-5 for the last 5 iterations
2. **Standard Deviation Limit**: Std Dev $<$ 1E-5 for the last 5 iterations

To visually confirm convergence we can plot the kinetic energy against the iteration:

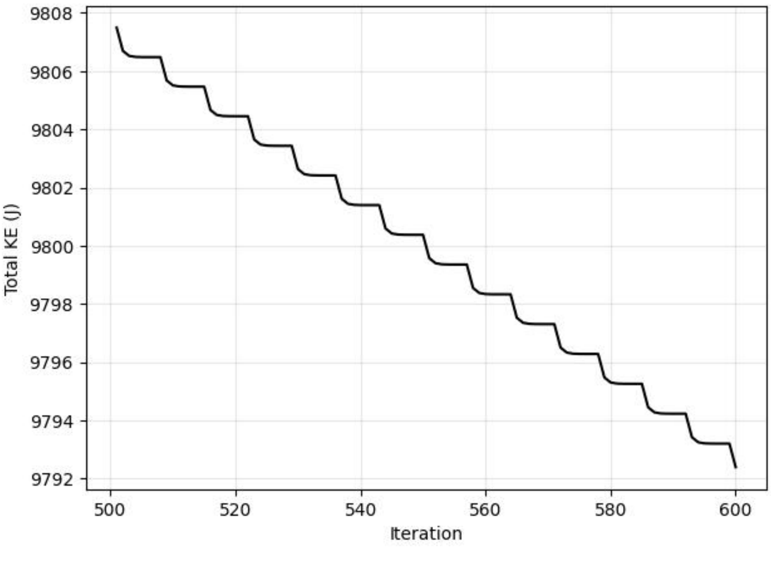

Figure 4.1: Convergence of the KE at every timestep for Hexa Mesh, 2nd order interpolator

A timestep of 0.02 s was selected. The associated Courant number should be lower than the CFL limit to guarantee stability. We can verify that the maximum Courant number is 0.82 (for the L-mesh). In the case of an explicit time-advancement scheme the CFL limit should be 1, so in our case $C < CFL$. But we are using an implicit scheme, for which the CFL is greater than 1. So we are confident that stability is more than guaranteed.

# 5. EXPERIMENT MATRIX

## 5.1. Interpolation Schemes

The following convection interpolation schemes were tested:

1. **1st Order**: 1st order upwind scheme
2. **2nd Order**: 2nd order upwind scheme
3. **MUSCL**: hybrid MUSCL third-order/central-differencing scheme

Generally we expect the lower order schemes to be faster but to introduce more numerical diffusion than the higher order schemes.

## 5.2. Meshes

A total of five meshes were studied in this homework:

1. **Hexa**: generated by Automatic 2D mesher
2. **Tetra**: generated by Automatic 2D mesher
3. **Poly**: generated by Automatic 2D mesher
4. **Multi-Polar**: generated by Direct Patch Meshing, the idea is to recreate a partially structured polar mesh to incorporate each vortex
5. **L-Mesh**: generated by Direct Patch Meshing, this is a silly mesh to recreate the letter L (as for "Lorenzo", or alternatively "Loser Mesh") and it is the only non-symmetric mesh

In table 5.1 are tabulated the main diagnostic metrics for each of the above meshes. The meshes are represented in figures 5.1-5.5.

| | **Hexa** | **Tetra** | **Poly** | **Multi-Polar** | **L-Mesh** |
|---|---|---|---|---|---|
| **Number of Cells** | 1024 | 946 | 1073 | 980 | 1013 |
| **Number of Faces** | 1984 | 1375 | 3088 | 1932 | 1978 |
| **Min Volume Change** | 1.0 | 0.56 | 0.19 | 0.5 | 0.05 |
| **Max Skewness Angle** | 0.0° | 28.2° | 21.7° | 34.6° | 64.4° |

Table 5.1: Diagnostic metrics for the five meshes used in this homework

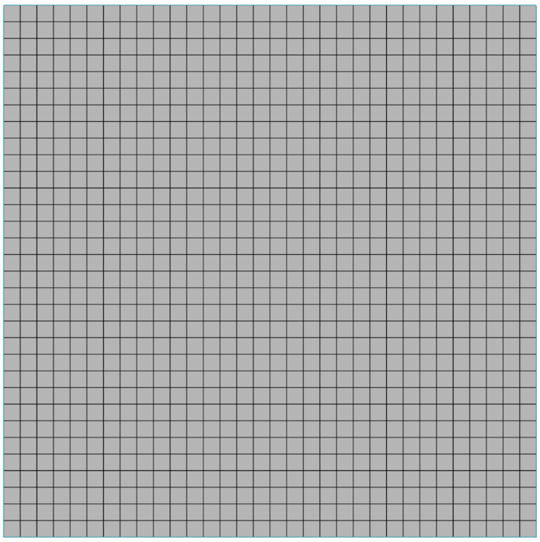

Figure 5.1: Hexa Mesh

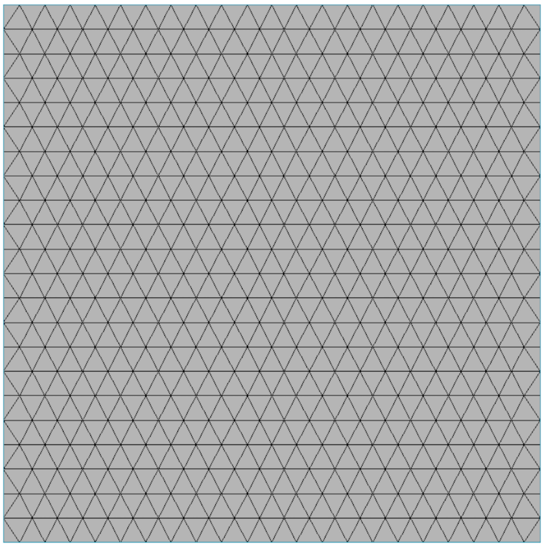

Figure 5.2: Tetra Mesh

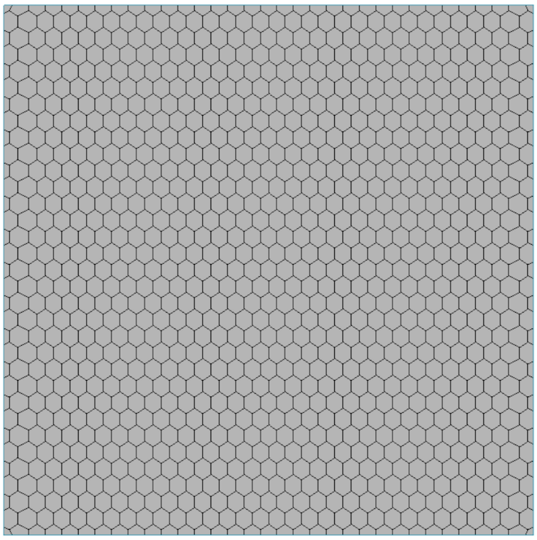

Figure 5.3: Poly Mesh

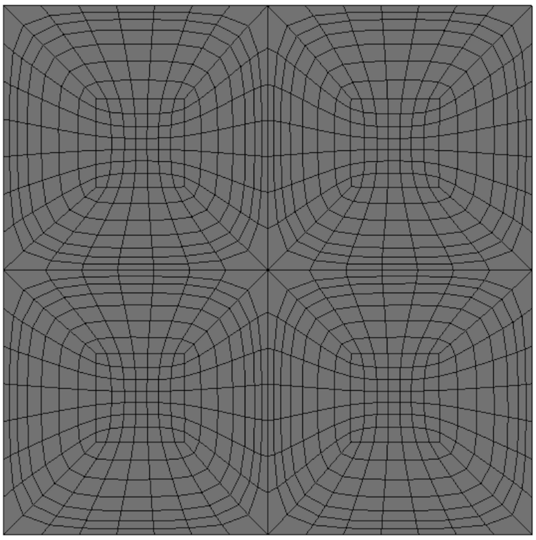

Figure 5.4: Multi-Polar Mesh

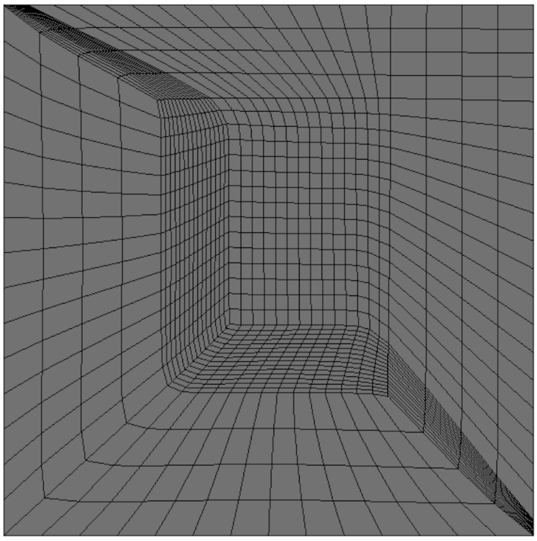

Figure 5.5: L-Mesh

# 6. RESULTS

The variable of interest is the (specific) kinetic energy (J/kg) of the fluid, defined as a function field:

$$K = \frac{1}{2}\left|\vec{v}\right|^2 = \frac{1}{2}\left(v_x^2 + v_y^2\right) \tag{6.1}$$

We reduce the dimensionality by integrating it over the whole domain mass obtaining the total kinetic energy of the system:

$$K_{tot} = \int_D K dm = \int_D K \rho dV \tag{6.2}$$

One can show that integrating the analytical velocity field for our initial conditions results in a total kinetic energy equal to $K_{tot} = \rho\pi^2$ (a complete derivation can be found in Appendix B). Using a density of 1000 $kg/m^3$ one gets an initial analytical value of $K_{tot} = 9869.6$ J.
All the meshes integrate the initial conditions correctly within a relative error of 0.5%.
I exported the values for $K_{tot}$ as a function of time. To get a sense of the ability of our scheme/mesh combination to conserve KE we can visualize the results using the following metric (conservation metric):

$$C = \frac{K_{tot}(t_f)}{K_{tot}(t_i)} \tag{6.3}$$

We set $t_i = 0s$ and $t_f = 10s$, results can be found in table 6.1 and are plotted in figure 6.1.

| | **Hexa** | **Tetra** | **Poly** | **Multi-Polar** | **L-Mesh** |
|---|---|---|---|---|---|
| **1st Order** | .36 | .37 | .29 | .25 | .19 |
| **2nd Order** | .95 | .89 | .93 | .79 | .57 |
| **MUSCL** | .98 | .86 | .97 | .86 | .68 |

Table 6.1: Conservation metric for each scheme-mesh combination in the test matrix

| **3rd Hexa** | **3rd Poly** | **2nd Hexa** | **2nd Poly** | **2nd Tetra** | **3nd Multi** | **3rd Tetra** | **2nd Multi** |
|---|---|---|---|---|---|---|---|
| .98 | .97 | .95 | .93 | .89 | .86 | .86 | .79 |
| **3rd L-Mesh** | **2nd L-Mesh** | **1st Tetra** | **1st Hexa** | **1st Poly** | **1st Multi** | **1st L-Mesh** | |
| .68 | .57 | .37 | .36 | .29 | .25 | .19 | |

Table 6.2: Conservation metric for each scheme-mesh, ranked from best to worst

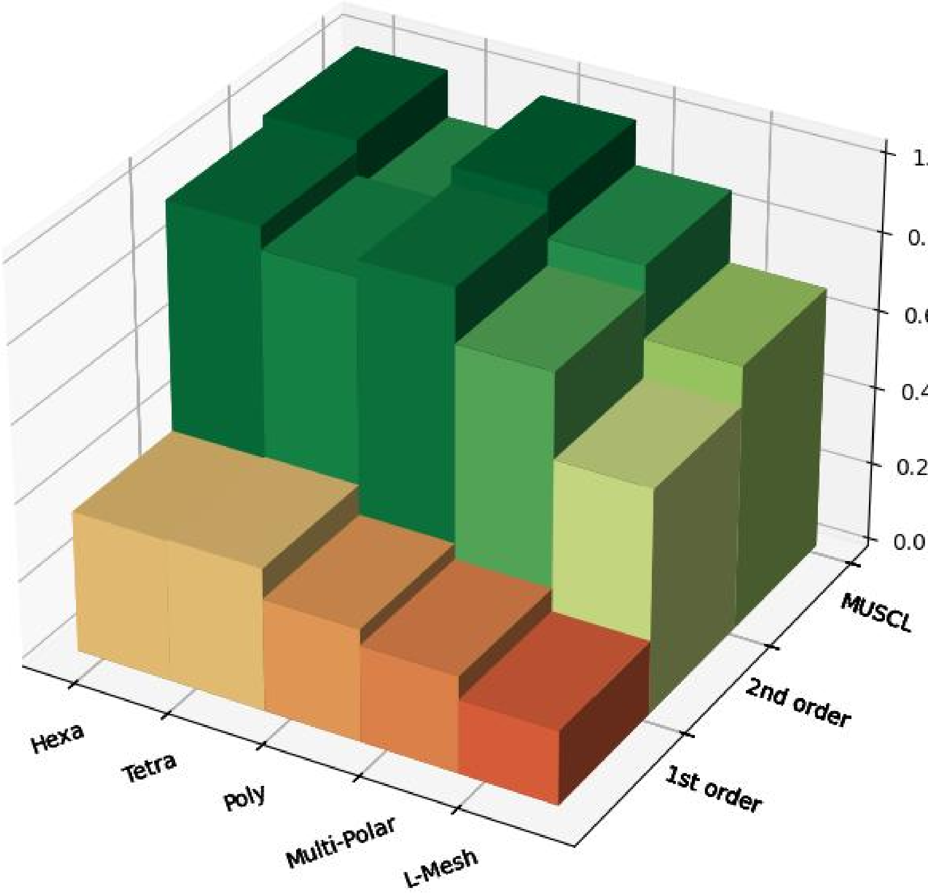

Figure 6.1: Conservation metric for each scheme-mesh combination

It is evident from this last plot that the conservation of kinetic energy is highly dependent on the scheme and way less dependent on the mesh. 1st order upwind interpolation is always outperformed by higher order schemes, no matter the mesh. Also a good quality mesh will outperform lower quality meshes given that they use the same interpolation scheme.

**What is the best mesh?**
Poly and Hexa outperform all the others.

**What is the best scheme?**
Overall the best scheme is the 3rd order MUSCL that generally outperforms the others (not in the case of the tetra-mesh for which the 2nd order upwind scheme is better than MUSCL).

**What is the worst mesh?**
The L-mesh is by far the worst. This is due to bad mesh quality, and lack of symmetry which is very important for this flow field. Between the high quality meshes the tetra-mesh is the one with poorest performance.

**What is the worst scheme?**
1st order upwind is by far the worst scheme.

We can also explicitly plot the evolution in time for every combination:

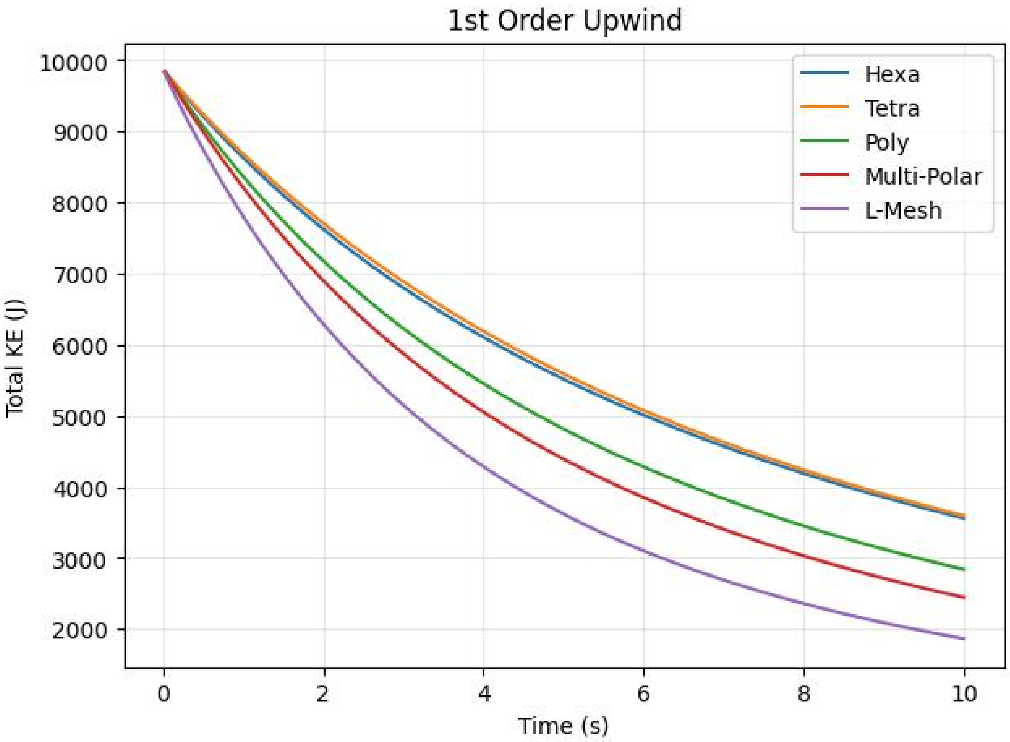

Figure 6.2: 1st order upwind scheme kinetic energy decay

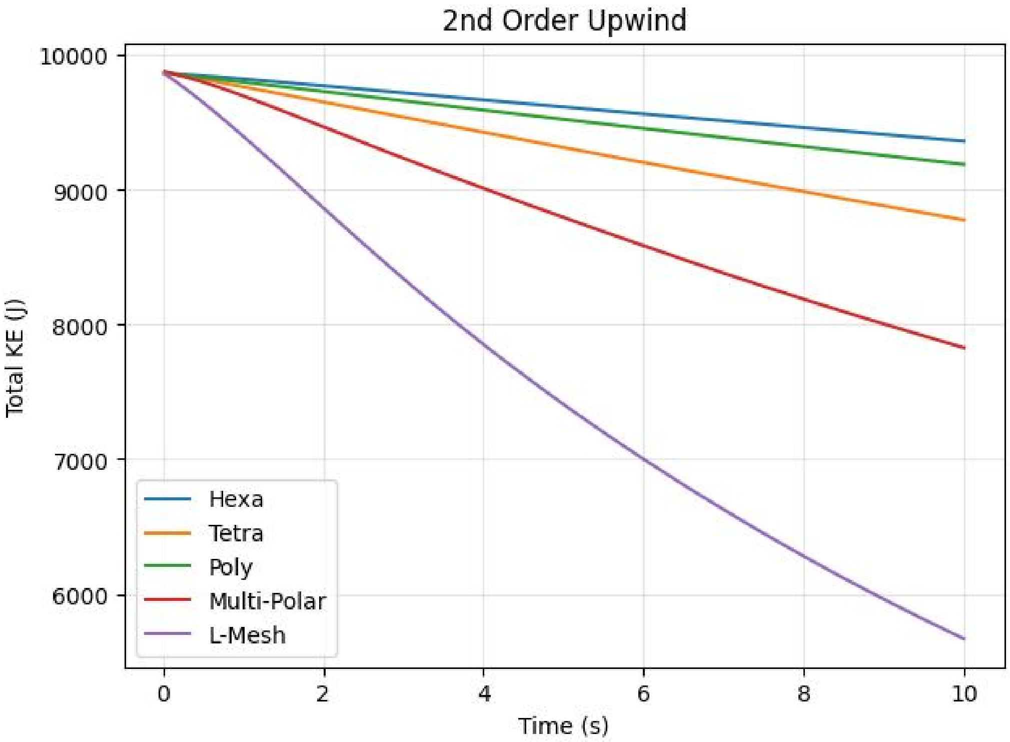

Figure 6.3: 2nd order upwind scheme kinetic energy decay

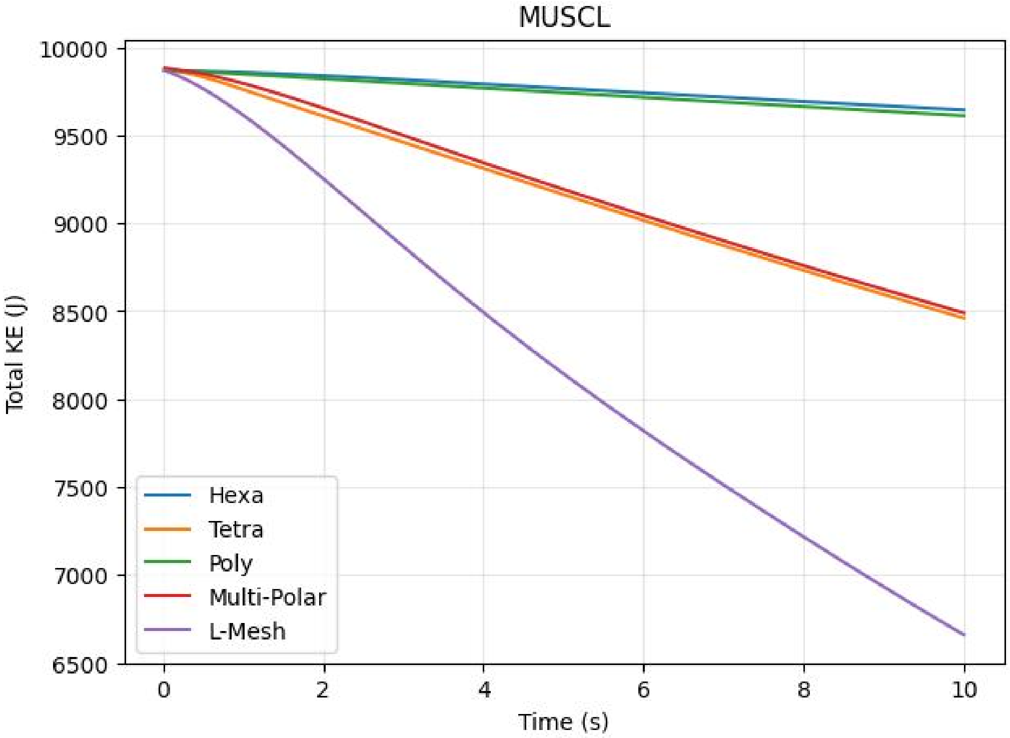

Figure 6.4: MUSCL scheme kinetic energy decay

Only the 1st order upwind scheme shows an exponential decay in time, all the other schemes behave linearly. It's also interesting to note how some meshes behave similarly for some interpolation schemes (like Tetra and Multi-polar using MUSCL or Tetra and Hexa for 1st order) but then show different performances for other schemes.

# Appendices

## A. Derivation of Initial Pressure Field for TG Vortices

The momentum equations for unsteady 2D flow are:

$$\text{Momentum-X: } \frac{\partial(\rho u)}{\partial t} + \frac{\partial(\rho u^2)}{\partial x} + \frac{\partial(\rho uv)}{\partial y} = -\frac{\partial P}{\partial x} + \frac{1}{Re}\left[\frac{\partial \tau_{xx}}{\partial x} + \frac{\partial \tau_{xy}}{\partial y}\right] \tag{A.1}$$

$$\text{Momentum-Y: } \frac{\partial(\rho v)}{\partial t} + \frac{\partial(\rho v^2)}{\partial y} + \frac{\partial(\rho uv)}{\partial x} = -\frac{\partial P}{\partial y} + \frac{1}{Re}\left[\frac{\partial \tau_{yy}}{\partial y} + \frac{\partial \tau_{xy}}{\partial x}\right] \tag{A.2}$$

Considering an incompressible ($\rho = const$) steady ($\frac{\partial}{\partial t} = 0$) and inviscid ($Re \rightarrow \infty$) flow, the equations become:

$$\text{Momentum-X: } \frac{\partial(u^2)}{\partial x} + \frac{\partial(uv)}{\partial y} = -\frac{1}{\rho}\frac{\partial P}{\partial x} \tag{A.3}$$

$$\text{Momentum-Y: } \frac{\partial(v^2)}{\partial y} + \frac{\partial(uv)}{\partial x} = -\frac{1}{\rho}\frac{\partial P}{\partial y} \tag{A.4}$$

Since we know the velocity field we can easily compute the derivatives found in the LHS of equations (3) and (4). This will prodive a system of 2 PDEs on the pressure field.

$$u(x,y) = sin(x)cos(y) \tag{A.5}$$

$$v(x,y) = -cos(x)sin(y) \tag{A.6}$$

$$\frac{\partial(u^2)}{\partial x} = 2cos^2(y)sin(x)cos(x) \tag{A.7}$$

$$\frac{\partial(uv)}{\partial y} = -cos^2(y)sin(x)cos(x) + sin^2(y)sin(x)cos(x) \tag{A.8}$$

$$\frac{\partial(v^2)}{\partial y} = 2cos^2(x)sin(y)cos(y) \tag{A.9}$$

$$\frac{\partial(uv)}{\partial x} = -cos^2(x)sin(y)cos(y) + sin^2(x)sin(y)cos(y) \tag{A.10}$$

Substituting (5)-(10) into (3) and (4) we find the following:

$$\text{Momentum-X: } -\frac{1}{\rho}\frac{\partial P}{\partial x} = sin(x)cos(x) = f(x) \tag{A.11}$$

$$\text{Momentum-Y: } -\frac{1}{\rho}\frac{\partial P}{\partial y} = sin(y)cos(y) = f(y) \tag{A.12}$$

Equations (11) and (12) tell us that $\frac{\partial P}{\partial x}$ is a function of $x$ only, and $\frac{\partial P}{\partial y}$ is a function of $y$ only. Therefore the two-variable scalar field has to be of the form $P(x,y) = g(x) + h(y)$, with $g$ and $h$ two unknown functions. With this information (11) and (12) become two uncoupled first order ODEs:

$$\text{Momentum-X: } -\frac{1}{\rho}\frac{\partial g}{\partial x} = sin(x)cos(x) \tag{A.13}$$

$$\text{Momentum-Y: } -\frac{1}{\rho}\frac{\partial h}{\partial y} = sin(y)cos(y) \tag{A.14}$$

Since:

$$\int sin(z)cos(z)dz = -\frac{1}{2}cos^2(z) + C \tag{A.15}$$

we find:

$$g(x) = \frac{\rho}{2}cos^2(x) + C_1 \tag{A.16}$$

$$h(y) = \frac{\rho}{2}cos^2(y) + C_2 \tag{A.17}$$

And finally:

$$P(x,y) = g(x) + h(y) = \frac{\rho}{2}\left[cos^2(x) + cos^2(y)\right] + C \tag{A.18}$$

# B. Analytical Integration of Kinetic Energy Field

By definition:

$$K_{tot} = \int_D K\rho dV = \frac{1}{2}\rho \int_D (v_x^2 + v_y^2) dV \tag{B.1}$$

We now that the initial velocity field is:

$$v_x(x, y) = sin(x)cos(y) \tag{B.2}$$

$$v_y(x, y) = -cos(x)sin(y) \tag{B.3}$$

But, given a constant cell height of 1:

$$\int_D (v_x^2 + v_y^2) dV = \int_{-\pi}^{\pi}\int_{-\pi}^{\pi} (v_x^2 + v_y^2) dxdy = 2\int_{-\pi}^{\pi}\int_{-\pi}^{\pi} sin^2(x)cos^2(y)dxdy = 2\pi^2 \tag{B.4}$$

Finally:

$$K_{tot} = \frac{1}{2}\rho \int_D (v_x^2 + v_y^2) dV = \rho\pi^2 \tag{B.5}$$

# C. Code

All the code can be found in this public GitHub Repository.